

## Temperature Effects on a Hydroxyapatite Precursor Solution

Adriyan S. Milev,<sup>\*,†</sup> G. S. Kamali Kannangara,<sup>†</sup> Besim Ben-Nissan,<sup>‡</sup> and Michael A. Wilson<sup>†</sup>

College of Science, Technology and Environment, University of Western Sydney, Locked Bag 1797, Penrith South DC 1797, Australia, and Department of Chemistry, Materials and Forensic Science, University of Technology, Sydney, P.O. Box 123, Sydney 2007, Australia

Received: June 2, 2003; In Final Form: March 4, 2004

Multinuclear NMR spectroscopy has been used to monitor synthesis of hydroxyapatite (HAp) from diethyl hydrogen phosphonate and calcium diethoxide in solution at two different temperatures. Acetyl 2-hydroxyethyl phosphonate, bis(2-hydroxyethyl) phosphonate, and acetyl ethyl phosphonate have been identified for the first time in this reaction solution as intermediates. The formation of these compounds is shown to be crucial in controlling the phase purity of the final hydroxyapatite product. A possible mechanism for the formation of acetyl 2-hydroxyethyl phosphonate is discussed.

### 1. Introduction

Hydroxyapatite (HAp) has been commonly used to repair missing, damaged, and diseased mineral tissues. Early work shows that while biphasic sol–gel HAp products are easily made, monophasic hydroxyapatite  $[\text{Ca}_{10}(\text{PO}_4)_6(\text{OH})_2]$  powders and coatings are more difficult to produce.<sup>1,2</sup> For example, it has been reported that synthesis from stoichiometric ratio of alkoxides only or mixed salt–alkoxide sol–gel systems produce impure hydroxyapatite accompanied by a second phase of calcium oxide.<sup>3–5</sup> Further investigations into the process showed that the time period between the mixing of precursors and heating to remove the solvent, which was referred to as “aging time”, could significantly alter the composition of the product.<sup>6–8</sup> Thus, for stoichiometric amounts of calcium diethoxide and triethyl phosphite ( $\text{Ca/P} = 1.67$ ) it takes about 16 h or more to form a mixture of stable intermediate compounds, which after thermal decomposition results in single-phase HAp.<sup>9,10</sup> If time periods of less than 16 h are employed, then the product is a mixture of HAp and calcium oxide. A phase evolution map for apatite formation considering temperature and time has been proposed by Liu et al.<sup>11</sup> In that report, the HAp phase purity map was produced by examining the HAp phase composition of a series of samples aged at various temperatures and times, followed by calcinations. However, no attempts have been made to characterize the intermediates in the precursor solution mixtures.

Likewise, in investigations with sol–gel methods using diethyl hydrogen phosphonate (DHP) and calcium salts and the existing sol–gel procedures suitable for HAp preparation we have shown that reaction conditions influence the purity of the hydroxyapatite product.<sup>12,13</sup> However, as with the synthesis from triethyl phosphite, little is known or reported about intermediates.

In the current work, we monitor the formation of phosphorus-containing species at two different temperatures (25 and 70 °C) by using nuclear magnetic resonance (NMR) spectroscopy to elucidate mechanism and the role of intermediate species on

HAp phase formation. It is shown that diethyl hydrogen phosphonate in the presence of calcium diethoxide, ethylene glycol, and acetic acid undergoes ligand substitution reactions, which influence HAp phase precipitation.

### 2. Experimental Procedure

**Reaction Solutions.** Solutions were prepared by dissolving ( $1.135 \times 10^{-3}$  mol) of calcium diethoxide (Kojundo Chemical Lab., Japan, >99% purity) in a solvent containing 1:1 molar ratio of ethylene glycol (Fluka, >99.5% purity) and acetic acid (Sigma >99.7% purity). When the calcium diethoxide was completely dissolved, a stoichiometric quantity of diethyl hydrogen phosphonate (DHP) ( $6.81 \times 10^{-4}$  mol, Sigma >98% purity) was added directly into the solution with stirring. The total volume of the solution was approximately 2 mL. Because of the hygroscopic nature of calcium diethoxide, the preparation was conducted in a glovebox containing purified dry nitrogen. The effect of temperature on the reaction was studied at ambient temperature (25 °C) up to 384 h and at 70 °C up to 96 h. A white precipitate was formed after 40–48 h of heating at 70 °C. After a fixed period of time for both solutions (48 h), reaction products were solidified by evaporation at 130 °C in a Petri dish. Hydroxyapatite samples were then obtained after firing of the precursor powders at 700 °C for 2 h.

**NMR Spectroscopy.** One-dimensional (1D) NMR spectra were acquired using a Bruker DRX-300 spectrometer operating at 300 MHz for protons ( $^1\text{H}$ ), 75.5 MHz for carbons ( $^{13}\text{C}$ ), and 121.5 MHz for phosphorus ( $^{31}\text{P}$ ) nuclei at 27 °C. The chemical shifts ( $\delta$ ) in the case of  $^1\text{H}$  and  $^{13}\text{C}$  were measured relative to an internal standard: methylene protons of ethylene glycol ( $-\text{CH}_2-$   $\delta = 3.68$  ppm) or methylene carbons of ethylene glycol ( $-\text{CH}_2-$  at  $\delta = 62.08$  ppm), respectively.  $^{31}\text{P}$  chemical shifts were measured relative to external 85%  $\text{H}_3\text{PO}_4$  standard ( $\delta = 0$  ppm). Proton, phosphorus, and carbon NMR spectra were obtained using 128 scans for  $^1\text{H}$  and  $^{31}\text{P}$  and 4096 scans for  $^{13}\text{C}$  with a recycle delay of 2 s. A two-dimensional (2D) NMR spectrum was acquired on Bruker Avance spectrometer operating at 400 MHz for protons ( $^1\text{H}$ ) and 161.9 MHz for phosphorus ( $^{31}\text{P}$ ) nuclei by heteronuclear multiple bond correlation (HMBC) spectroscopy. A filter delay corresponding to an average  $^1J_{\text{H-P}}$  of 638 Hz and a single evolution period of

\* Corresponding author. Telephone: +61 2 9685 9936. Fax: +61 2 9685 9915. E-mail: a.milev@uws.edu.au.

<sup>†</sup> University of Western Sydney.

<sup>‡</sup> University of Technology.

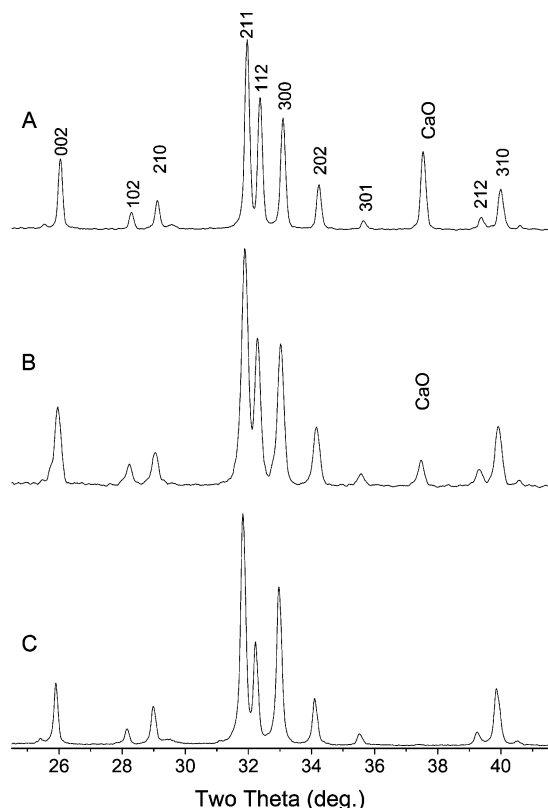


**Figure 1.** XRD patterns of hydroxyapatite obtained from solutions heated at two different temperatures for different times. All solutions were subsequently solidified at 130 °C and fired at 700 °C for 2 h. (A) Solution heated at 25 °C for 48 h. Note the intense peak of CaO phase. (B) Solution heated at 25 °C for 384 h. (C) Solution heated at 70 °C for 48 h.

250 ms corresponding to coupling constant of 4 Hz were employed to select long-range correlations. The  $^1\text{H}$ – $^{31}\text{P}$  HMBC spectra were recorded with gradient phase cycling.

Integration of the areas of the doublets in a 1D proton-coupled  $^{31}\text{P}$  spectrum was used to quantify the phosphorus-containing species obtained after heating at 48 h at 70 °C. The sum of the integrated areas was taken as 100%. The spectrum is not shown in the article.

**ATR FT-IR.** Solutions were also analyzed using a Nicolet Magna IR 560 FT-IR spectrometer. A germanium attenuated-total-reflectance (ATR) crystal was employed. The spectra were recorded between 4000 and 650  $\text{cm}^{-1}$  wavenumbers and consisted of 256 scans at 4  $\text{cm}^{-1}$  resolution.

**X-ray Diffraction.** Hydroxyapatite powders were analyzed on Siemens D-5000 diffractometer, employing Cu K $\alpha$  radiation (40 kV, 30 mA). The diffraction pattern was collected over the  $2\theta$  ranges 24.5–41.5° with acquisition time of 5.0 s at 0.02° step size.

### 3. Results and Discussion

**3.1. HAp Phase Evolution: 25 vs 70 °C.** Figure 1 presents X-ray patterns for HAp obtained from sols at 25 and 70 °C, allowing a 48-h time period between the time of mixing and heating to evaporate the solvents. Spectra were obtained on products that had been dried at 130 °C for 48 h and subsequently fired at 700 °C for 2 h. The HAp powders derived from solution at 25 °C contained a large amount of calcium oxide phase (at  $2\theta = 37.5^\circ$ ) in addition to hydroxyapatite (Figure 1 A). Similar product profile was found even when the solution was kept at ambient temperature for 384 h (Figure 1 B). Increasing the

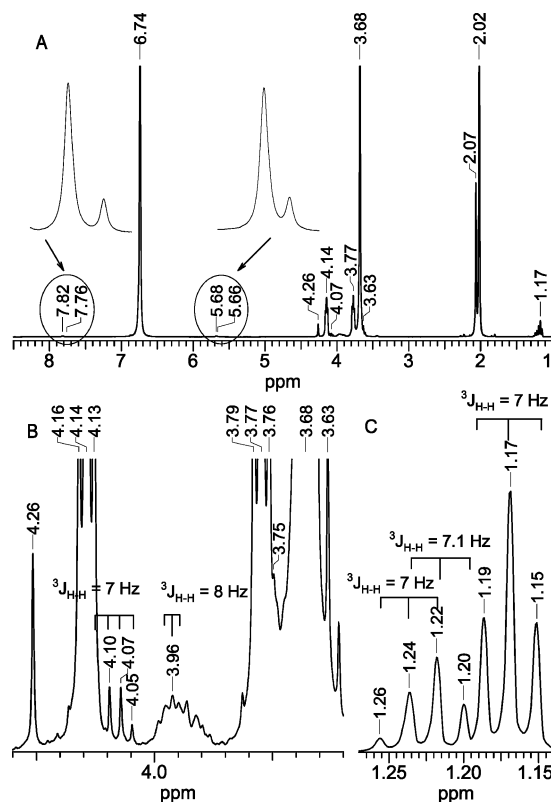


**Figure 2.** Proton NMR spectra of solution. (A) Heated at 70 °C for 48 h. (B and C) Expanded methylene and methyl regions of spectrum A. Splitting patterns of some weaker resonances are given.

temperature to 70 °C afforded monophasic hydroxyapatite with no other phases and impurities such as calcium oxide (Figure 1 C).

**3.2. Chemical Shifts and Assignments of NMR Spectral Data for Solution at 70 °C.** Ethanol was produced in situ during the ligand substitution reaction of DHP and calcium diethoxide. Proton NMR spectroscopic data (Figure 2A–C) revealed that one of the side reactions in the solution was esterification between acetic acid and the hydroxyl group in ethylene glycol and ethanol molecules.

In the methyl region, the triplet centered at 1.17 ppm ( $^3J_{\text{H-H}} = 7.0$  Hz) was assigned to methyl protons of ethanol. The ethanol methylene protons appeared as a quartet at 3.65 ppm ( $^3J_{\text{H-H}} = 7.0$  Hz), which were to some extent covered by the methylene protons of ethylene glycol at 3.68 ppm. The quartet at 4.085 ppm ( $^3J_{\text{H-H}} = 7.0$  Hz) partly obscured by a peak at 4.14 ppm, (Figure 2 B) was assigned to the methylene protons of ethyl acetate. The methyl protons next to methylene protons appeared as a triplet at 1.22 ppm ( $^3J_{\text{H-H}} = 7.1$  Hz). In the methylene region, the two sets of triplet peaks at 3.77 and 4.14 ppm were mutually spin-coupled to each other ( $^3J_{\text{H-H}} = 4.8$  Hz). These were assigned to two methylene groups of asymmetric 2-hydroxyethyl acetate ester. The methylene protons that were closer to the acetate group were deshielded and therefore shifted downfield (4.14 ppm) relative to the methylene protons next to hydroxyl group (3.77 ppm). The singlet at 4.26 ppm was assigned to two  $-\text{CH}_2\text{CH}_2-$  methylene groups of 2-(acetyloxy)ethyl acetate ester, which have a symmetrical chemical environment. All esters showed methyl proton resonances originating from their respective acetate groups at about 2.07 ppm.

Protons directly bonded to phosphorus nuclei appeared as two doublets centered at 6.75 ppm ( $^1J_{\text{H-P}} = 642$  Hz) and at 6.71 ppm ( $^1J_{\text{H-P}} = 630$  Hz). These resonances were different from

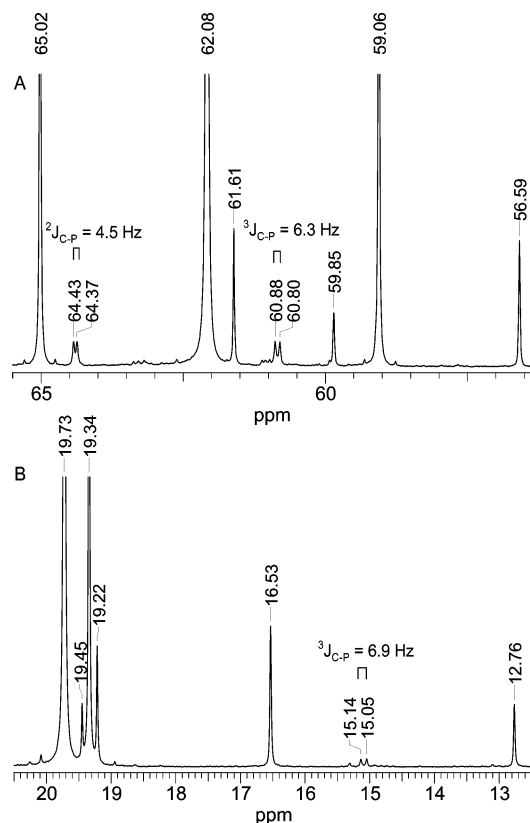


**Figure 3.** Expanded  $^{13}\text{C}\{\text{H}\}$  spectra of the precursor solution heated at 70 °C for 48 h. (A) Methylene region. (B) Methyl region. Carbon–phosphorus couplings are shown.

that of the diethyl hydrogen phosphonate and could have originated from at least two phosphonate species formed during heating. Another striking feature was the appearance of multiplets having maxima at about 3.96, 3.92, and 3.75 ppm. The  $^1\text{H}$ – $^{31}\text{P}$  2D NMR revealed that these signals were associated with phosphorus-containing intermediates. Some of the protons belonging to the new phosphorus-containing intermediates were obscured by the protons of ethylene glycol, acetic acid, and the esters (see overlaps in Figure 2B,C) because of similarities in their chemical environments. However, carbon-13 proton-decoupled  $^{13}\text{C}\{\text{H}\}$  NMR revealed  $^{13}\text{C}$ – $^{31}\text{P}$  connectivities in the methylene and methyl regions (Figure 3). The peaks at 60.84 ppm (doublet,  $^3J_{\text{C-P}} = 6.3$  Hz) and 64.40 ppm (doublet,  $^2J_{\text{C-P}} = 4.5$  Hz) originated from three- and two-bond carbon–phosphorus couplings of newly formed phosphorus-containing compounds (Figure 3 A). The magnitude of the coupling constant is affected by the substituents attached to the respective carbons. For example, electron-donating group increases the  $^3J_{\text{C-P}}$  while electron-withdrawing group decreases the  $^2J_{\text{C-P}}$  values.<sup>14</sup> In the aliphatic region, a doublet at 15.09 ppm ( $^3J_{\text{C-P}} = 6.9$  Hz) was assigned to ethoxy methyl carbon coupled to phosphorus nucleus (Figure 3B).

Two-dimensional HMBC  $^1\text{H}$ – $^{31}\text{P}$  NMR experiments were employed to identify the long-range connections of protons associated with each phosphorus-containing compound and thus their identity. Accordingly, by extracting 1D rows at the resonance frequency of each phosphorus-containing compound, it was possible to link the coupled protons to the phosphorus atoms in the same molecule (Figures 4 and 5).

Three proton ( $^1\text{H}$ ) cross sections from HMBC  $^1\text{H}$ – $^{31}\text{P}$  2D spectra were taken along the length of the phosphorus chemical shifts through signals at 4.61 P{H}, 5.52 P{H}, and 4.92 P{H} ppm, respectively (Figure 5A–C). Compound A with  $^{31}\text{P}\{\text{H}\}$

resonance at 4.61 ppm showed proton directly attached to phosphorus (doublet at 6.71 ppm,  $^1J_{\text{H-P}} = 630$  Hz) and long-range phosphorus–proton interconnectivities in methylene (triplet at 3.92 ppm,  $^3J_{\text{H-H}} = 6$  Hz) and in methyl regions. The latter were represented by methyl protons participating in an ethoxy group (triplet at 1.25 ppm,  $^3J_{\text{H-H}} = 4$  Hz) and by methyl protons due to acetyl groups (doublet at 2.05 ppm,  $^4J_{\text{H-P}} = 24$  Hz). The presence of the ethoxy group bonded to a phosphorus nucleus was further supported by the 1D  $^{13}\text{C}$  spectral data shown in Figure 3B (doublet at 15.09 ppm,  $^3J_{\text{C-P}} = 6.9$  Hz). Structure A in Figure 6 gives the proposed configuration of acetyl ethyl phosphonate. It was about 14% yield of the intermediates present.

The major phosphorus-containing compound B, with a  $^{31}\text{P}$ –{H} resonance at 5.52 ppm (Figures 4 and 5B), showed a doublet at 6.76 ppm ( $^1J_{\text{H-P}} = 642$  Hz) due to proton directly attached to phosphorus and two different resonances in the methylene region, a strong peak centered at 3.97 (triplet,  $^3J_{\text{H-H}} = 8$  Hz), and a weak peak at about 3.74 ppm. The doublet in the methyl region at 2.055 ppm ( $^4J_{\text{H-P}} = 20$  Hz) was due to long-range coupling between phosphorus and proton. The latter doublet originates from methyl protons of acetate ligands, which are chemically equivalent, spin–spin-coupled to phosphorus nuclei. These findings suggested that one of the ethoxy groups of the initial DHP has been substituted by an acetate ligand. The presence of methylene protons indicated that the other ligand might be  $-\text{OCH}_2\text{CH}_2\text{OH}$ , with protons coupled to phosphorus nuclei via  $^3J_{\text{P-H}}$ . These spectral data together with phosphorus–carbon interactions revealed in  $^{13}\text{C}$  spectra (doublet due to P–O–C at 64.40 ppm,  $^2J_{\text{C-P}} = 4.5$  Hz, and doublet due to P–O–C–C at 60.84 ppm,  $^3J_{\text{C-H}} = 6.3$  Hz) allowed the identification of the chemical structure of the major phosphonate intermediate (approximately 71%) as acetyl 2-hydroxyethyl phosphonate (Figure 6B).

The splitting of the resonances at about 2.05 ppm for structures A and B is worth mentioning. The magnitude of the long-range proton–phosphorus coupling constants observed in the NMR spectra could be as a consequence of the  $\pi$ -electron conjugation extending over the six-membered ring in the presence of  $\text{Ca}^{2+}$  as shown in Figure 6.<sup>15</sup> It is important to note that the shifts and spin–spin couplings were obtained in the presence of  $\text{Ca}^{2+}$ , which may significantly change the magnitude of the coupling constants compared with the coupling patterns of free ligands.<sup>16,17</sup>

The large splitting constant seen in the proton cross section at 4.92 ppm  $^{31}\text{P}\{\text{H}\}$  resonance indicated that the third phosphorus-containing species also had proton directly attached to phosphorus nucleus (doublet at 6.75 ppm,  $^1J_{\text{H-P}} = 640$  Hz). The other phosphorus–proton spin interactions were observed in the methylene region only. These were represented by a triplet at 4.07 ppm ( $^3J_{\text{H-H}} = 6$  Hz) and faint resonances at about 3.94 ppm. These resonances and spin–spin couplings have been assigned to bis(2-hydroxyethyl) phosphonate (Figure 6C). It was present in approximately 13% yield. The proton-coupled  $^{31}\text{P}$  spectrum (not shown in the article) revealed the presence of a weak doublet centered at 2.66 ppm ( $^1J_{\text{P-H}} = 629$  Hz, at pH 3.6). This was assigned to the fourth phosphorus-containing compound, phosphonic acid. Spiking the solution with a trace amount of commercial phosphonic acid confirmed the peak assignment. The amount of the phosphonic acid (D) was approximately 2%.

**3.3. Ligand Substitutions at 70 °C.** The results suggested that a multicomponent mixture consisting of 2-hydroxyethyl acetate, 2-(acetyloxy)ethyl acetate, water, ethanol, and ethyl

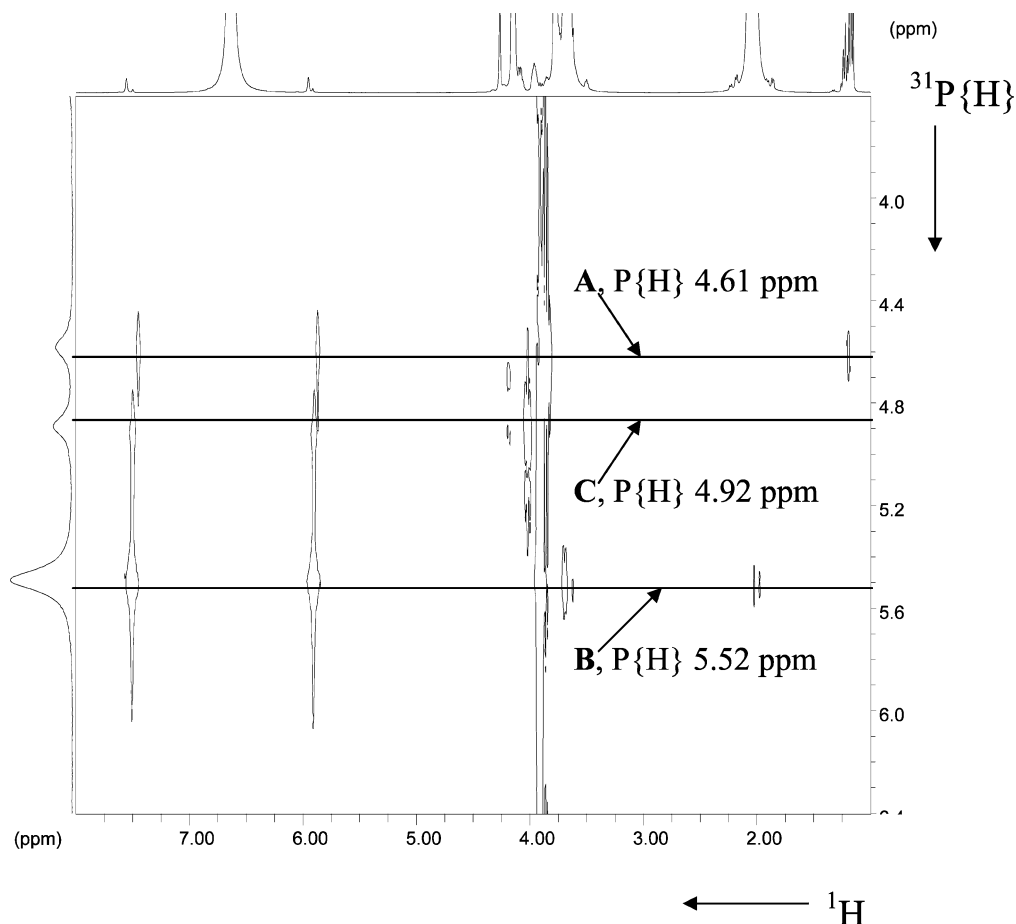
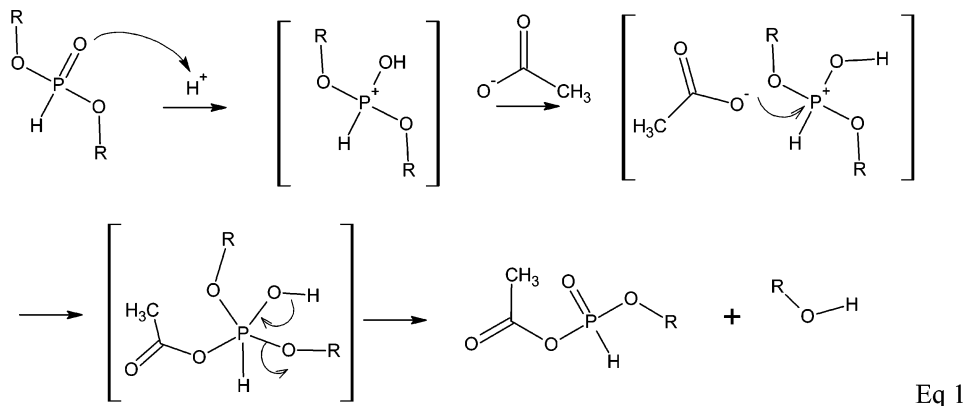


**Figure 4.** Gradient  $^1\text{H}$ – $^{31}\text{P}$  HMBC NMR spectrum of solution heated for 48 h at 70 °C obtained using a spectrometer operating at 400 MHz. The experiment was optimized for couplings of  $\sim 4$  Hz. One-bond couplings were filtered by 638 Hz filter. The proton-decoupled  $^{31}\text{P}\{\text{H}\}$  spectrum is given along the Y-axis.

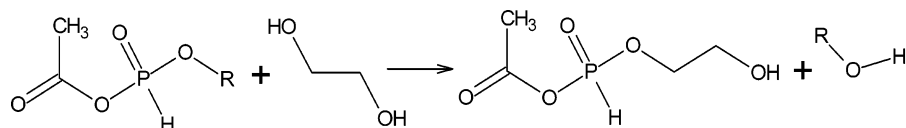
acetate was formed during reaction at 70 °C. The first step of ligand substitution would be reversible protonation of the phosphoryl group, resulting in an increase electron demand on the phosphorus atom.<sup>18,19</sup> The increased electron demand facilitates the attack by an acetate ion. The intermediate rearranges to form the more stable  $\text{P}=\text{O}$  bond with the elimination of a molecule of ethanol (eq 1, where R is an  $\text{CH}_2\text{-CH}_3$  group).<sup>20</sup>

These reactions could continue in the acidic medium. The intermediate acetyl ethyl phosphonate undergoes further attack by a glycol ligand that eliminated the second ethoxy group. This resulted in the synthesis of acetyl 2-hydroxyethyl phosphonate, the most abundant phosphonate formed during 48-h time period at 70 °C (eq 2).

It is thought that the ligand substitution could be facilitated by the presence of metal ions that act as a general acid catalyst



Eq 1



Eq 2



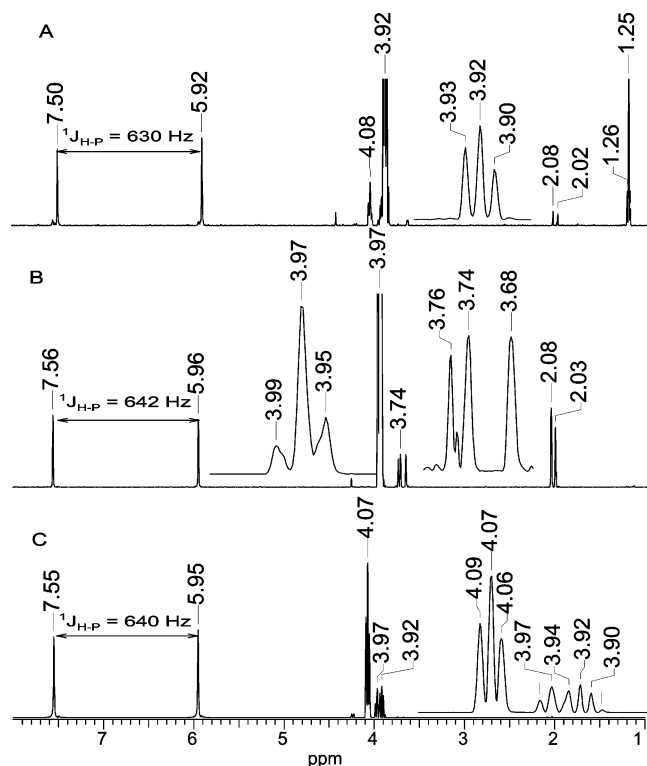


**Figure 5.** Three  $^1\text{H}$  cross sections from  $^1\text{H}$ - $^{31}\text{P}$  HMBC spectrum shown in Figure 4. (A) Cross section through signal at  $^{31}\text{P}\{\text{H}\} = 4.61$  ppm. (B) Cross section through  $^{31}\text{P}\{\text{H}\} = 5.52$  ppm. (C) Cross section through  $^{31}\text{P}\{\text{H}\} = 4.92$  ppm.

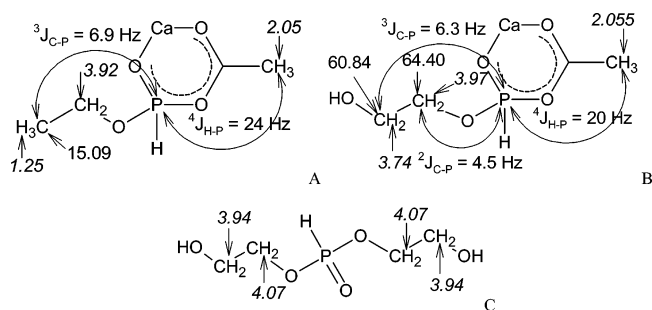


**Figure 6.** Chemical structures of the phosphorus-containing species that were formed at  $70^\circ\text{C}$  after 48 h. (A) Acetyl ethyl phosphonate. (B) Acetyl 2-hydroxyethyl phosphonate. (C) Bis(2-hydroxyethyl) phosphonate. Proton chemical shifts are given in italics. Structures A and B representing the acetyl phosphonates are given as calcium complexes.

(that is, like the proton). The calcium ions could coordinate to the oxygen on the phosphoryl group, thus increasing susceptibility to nucleophilic attack on phosphorus, possibly to the ethoxy group, or both, thus assisting its departure.<sup>21</sup> The formation of these phosphonate intermediates afforded an opportunity to form several chelates with the calcium ions present in the solution possibly through ring formation.<sup>22–27</sup>

It is clear that complexes of the types shown in Figure 6 have a 1:1 stoichiometry between calcium and phosphorus, and thus phosphorus is locked with calcium en route to hydroxyapatite. Thus the presence of these intermediates could be the key to forming stoichiometric apatite. Phosphorus-31 NMR of the reaction products in *absence* of calcium precursor revealed that almost complete hydrolysis of the initial DHP was achieved after 24 h at  $70^\circ\text{C}$ , giving rise to phosphonic acid ( $\text{H}_3\text{PO}_3$ ). The role of calcium ions in the ligand substitution process is

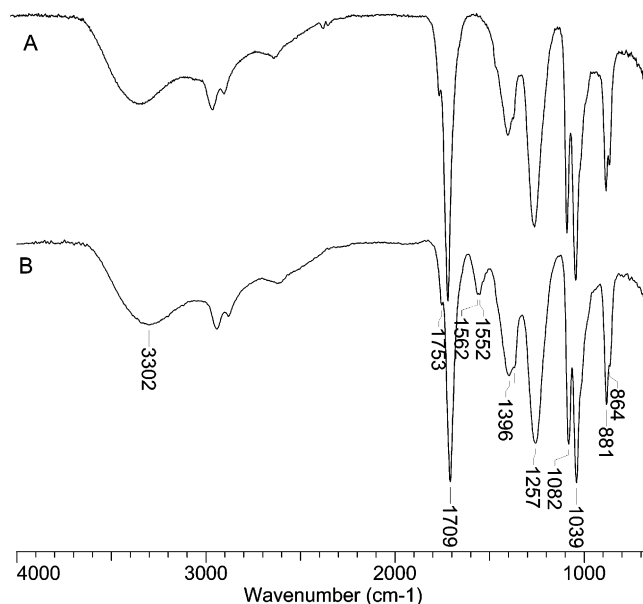


**Figure 7.** ATR-FTIR reflectance spectra of the precursor solution 48 h at  $70^\circ\text{C}$ . (A) In absence of calcium diethoxide. (B) In presence of calcium precursor. Note the appearance of two peaks at around  $1560\text{ cm}^{-1}$  because of formation of calcium alkoxo-acetate or calcium acetate.

**TABLE 1: Transformation of the Initial DHP as a Function of Time and Temperature ( $25$  and  $70^\circ\text{C}$ )<sup>a</sup>**

time (h)	temp ( $^\circ\text{C}$ )	A (%)	B (%)	C (%)	D (%)
24	25	0	3.5	0	0
	70	12.4	72.9	7.8	2.3
48	25	0	6.7	0	0
	70	13.6	71.4	12.9	2.1
96	25	2.0	12.5	0	0
	70	14.0	71.1	13.2	1.7
192	25	2.9	21.0	0	0
	70				
384	25	5.6	36.1	0	0
	70				

<sup>a</sup> The formation of acetyl ethyl phosphonate (A), acetyl 2-hydroxyethyl phosphonate (B), bis(2-hydroxyethyl) phosphonate (C), and phosphonic acid ( $\text{H}_3\text{PO}_3$ ) (D) was observed.

therefore much more important than acting as a catalyst. It is clear that  $\text{Ca}^{2+}$  ions stabilize the acetyl phosphonates as chelates.

Infrared spectra of solution without (Figure 7A) and with calcium diethoxide (Figure 7B) at  $70^\circ\text{C}$  for 48 h gave further evidence that acetate ions acted as ligands and changed the calcium diethoxide precursor at a molecular level. The main difference between both solutions was that the spectrum in the presence of calcium diethoxide showed two peaks at  $1562$  and  $1552\text{ cm}^{-1}$  (Figure 7B). These vibrations could be attributed to acetate ligands coordinated to calcium ions.<sup>28,29</sup>

### 3.4. Comparison of Products at Different Temperatures.

A solution containing diethyl hydrogen phosphonate and calcium diethoxide in the mixed solvent system containing ethylene glycol and acetic acid was kept at ambient temperature ( $25^\circ\text{C}$ ) for 384 h. This solution was also analyzed using NMR spectroscopic techniques (as described earlier for  $70^\circ\text{C}$  samples) to gather data on the relative concentrations and structure(s) of phosphonate intermediates. The integration of the areas under the respective  $^{31}\text{P}$  resonances provided the relative abundance of the phosphonate species (Table 1).

The results from  $^{31}\text{P}$  NMR spectroscopy revealed that two phosphonate species, acetyl ethyl phosphonate (A) and acetyl 2-hydroxyethyl phosphonate (B), 5.6 and 36.1%, respectively, were formed after 384 h at  $25^\circ\text{C}$ , but reactions were rather

slow. The bis(2-hydroxyethyl) phosphonate and phosphonic acid (C and D, respectively) were not present in detectable amounts even after 384 h. At 70 °C, the solution reached a state of equilibrium after 24 h, which was affirmed by the insignificant changes in relative concentrations of the phosphonate species. The concentrations of the major phosphonate acetyl 2-hydroxyethyl phosphonate (B) after 48 h were 6.7 and 71.4% at 25 and 70 °C, respectively. These data indicated a 10-fold increase in the reaction rate of the formation of acetyl 2-hydroxyethyl phosphonate.

**3.5. Phase Purity.** The formation of structures shown in Figure 6 may be an explanation as to why monophasic HAP was formed at 70 °C. At 25 °C, the structures were in much less concentration and the volatile DHP precursor remained mostly unchanged. Therefore, more phosphorus was uncomplexed and, hence, was lost by evaporation on heating to 700 °C, thus increasing Ca to P ratio that led to appearance of CaO in final HAP phase. In contrast, at relatively higher temperatures (70 °C), much larger amounts of structures A and B were formed, and the hydroxyapatite produced exhibited higher stoichiometric purity.

#### 4. Conclusions

1. Acetyl ethyl phosphonate (A), acetyl 2-hydroxyethyl phosphonate (B), bis(2-hydroxyethyl) phosphonate (C), and phosphonic acid (D) have been identified for the first time in solutions of diethyl hydrogen phosphonate and calcium diethoxide in stoichiometric ratios of ethylene glycol and acetic acid heated at 70 °C for 48 h. At 25 °C for 384 h, the reaction rate is slow and only low concentrations of intermediates A and B were observed, with C and D being absent.

2. Compounds A and B may form a complex with  $\text{Ca}^{2+}$ , which effectively locks up phosphate and reduces its loss during thermal treatment at 700 °C. Hence, under reaction conditions of 70 °C for 48 h followed by drying and heating to 700 °C monophasic hydroxyapatite is formed. In the absence or decreased amount of this complex, impure hydroxyapatite is produced containing phases of calcium oxide.

#### References and Notes

- (1) Layrolle, P.; Ito, A.; Tateishi, T. *J. Am. Ceram. Soc.* **1998**, *61*, 1421.
- (2) Weng, W.; Baptista, J. *Biomaterials* **1998**, *19*, 125.
- (3) Deptula, A.; Lada, W.; Olczak, T.; Borello, A.; Alvini, C.; di Bartolomeo, A. *J. Non-Cryst. Solids* **1992**, *147–148*, 537.
- (4) Masuda, Y.; Matubara, K.; Sakka, S. *J. Ceram. Soc. Jpn.* **1990**, *98*, 1266.
- (5) Lopatin, C.; Pizziconi, V.; Alford, T.; Laursen, T. *Thin Solid Films* **1998**, *326*, 227.
- (6) Chai, C.; Ben-Nissan, B. *J. Mater. Sci.: Mater. Med.* **1999**, *10*, 456.
- (7) Liu, D.; Troczynski, T.; Tseng, W. *Biomaterials* **2001**, *21*, 1721.
- (8) Liu, D.; Yang, Q.; Troczynski, T.; Tseng, W. *Biomaterials* **2002**, *23*, 1679.
- (9) Gross, K.; Chai, C.; Kannangara, G. S. K.; Ben-Nissan, B.; Hanley, L. *J. Mater. Sci.: Mater. Med.* **1998**, *9*, 839.
- (10) Chai, C.; Gross, K.; Ben-Nissan, B. *Biomaterials* **1998**, *19*, 2291.
- (11) Liu, D.; Troczynski, T.; Tseng, W. *Biomaterials* **2002**, *23*, 1227.
- (12) Ben-Nissan, B.; Green, D.; Kannangara, G. S. K.; Chai, C.; Milev, A. *J. Sol.-Gel Sci. Technol.* **2001**, *21*, 27.
- (13) Green, D.; Kannangara, G. S. K.; Milev, A.; Ben-Nissan, B. *Key Eng. Mater.* **2002**, *218–220*, 75.
- (14) Gray, G. *J. Am. Chem. Soc.* **1971**, *93*, 2132.
- (15) Cotton, F.; Schunn, R. *J. Am. Chem. Soc.* **1963**, *85*, 2394.
- (16) Kluger, R.; Wasserstein, P. *J. Am. Chem. Soc.* **1973**, *95*, 1071.
- (17) Kluger, R.; Wasserstein, P.; Nakaoka, K. *J. Am. Chem. Soc.* **1975**, *97*, 4298.
- (18) Doak, G.; Freedman, L. *Chem. Rev.* **1961**, *61*, 31.
- (19) Westheimer, F.; Huang, S.; Covitz, F. *J. Am. Chem. Soc.* **1988**, *110*, 181.
- (20) Mitchell, M.; Taylor, R.; Kee, T. *Polyhedron* **1998**, *17*, 433.
- (21) Houghton, R. *Metal Complexes in Organic Chemistry*; Cambridge University Press: Cambridge, 1979; pp 158–160.
- (22) Nagar, P. *Phosphorus Sulfur* **1993**, *79*, 207.
- (23) Matczak-Jon, E.; Kurzak, B.; Sawka-Dobrowolska, W.; Lejczak, B.; Kalafski, P. *J. Chem. Soc., Dalton. Trans.* **1998**, *1998*, 161.
- (24) Sigel, H.; Da Costa, C.; Song, B.; Carloni, P.; Gregan, F. *J. Am. Chem. Soc.* **1999**, *121*, 6248.
- (25) Sigel, H.; Kapinos, L. *Coord. Chem. Rev.* **2000**, *200–202*, 563.
- (26) Gibson, D.; Karaman, R. *J. Chem. Soc., Dalton Trans.* **1989**, *1*, 1911.
- (27) Hirschmann, R.; Yager, K.; Taylor, C.; Witherington, J.; Sprengeler, P.; Phillips, B.; Moore, W.; Smith, A. *J. Am. Chem. Soc.* **1997**, *119*, 8177.
- (28) Belamy, L. *The Infrared Spectra of Complex Molecules*, 3rd ed.; Chapman and Hall: London, 1975.
- (29) Nakamoto, K. *Infrared and Raman Spectra of Inorganic and Coordination Compounds*, 3rd ed.; Wiley-Interscience: New York, 1978; pp 232–233.